

# Neutrino mass bounds from DESI 2024 are relaxed by Planck PR4 and cosmological supernovae

Itamar J. Allali<sup>1,\*</sup> and Alessio Notari<sup>2,3,†</sup>

<sup>1</sup>*Department of Physics, Brown University, Providence, RI 02912, USA*

<sup>2</sup>*Departament de Física Quàntica i Astrofísica & Institut de Ciències del Cosmos (ICCUB),  
Universitat de Barcelona, Martí i Franquès 1, 08028 Barcelona, Spain.*

<sup>3</sup>*Galileo Galilei Institute for theoretical physics,  
Centro Nazionale INFN di Studi Avanzati Largo Enrico Fermi 2, I-50125, Firenze, Italy*

The recent DESI 2024 Baryon Acoustic Oscillations (BAO) measurements combined with the CMB data from the Planck 18 PR3 dataset and the Planck PR4+ACT DR6 lensing data, with a prior on the sum of the neutrino masses  $\sum m_\nu > 0$ , leads to a strong constraint,  $\sum m_\nu < 0.072$  eV, which would exclude the inverted neutrino hierarchy and put some tension on even the standard hierarchy. We show that actually this bound gets significantly relaxed when combining the new DESI measurements with the HiLLiPoP + LoLLiPoP likelihoods, based on the Planck 2020 PR4 dataset, and with supernovae datasets. We note that the fact that neutrino masses are pushed towards zero, and even towards negative values, is known to be correlated with the so-called  $A_L$  tension, a mismatch between lensing and power spectrum measurements in the Planck PR3 data, which is reduced by HiLLiPoP + LoLLiPoP to less than  $1\sigma$ . We find  $\sum m_\nu < 0.1$  eV and  $\sum m_\nu < 0.12$  eV, with the supernovae *Pantheon+* and *DES-SN5YR* datasets respectively. The shift caused by these datasets is more compatible with the expectations from neutrino oscillation experiments, and both the normal and inverted hierarchy scenarios remain now viable, even with the  $\sum m_\nu > 0$  prior. Finally, we analyze neutrino mass bounds in an extension of  $\Lambda$ CDM that addresses the  $H_0$  tension, with extra fluid Dark Radiation, finding that in such models bounds are further relaxed and the posterior probability for  $\sum m_\nu$  begins to exhibit a peak at positive values.

## I. Introduction

Cosmological observations are at present the most promising way to detect for the first time the sum of neutrino masses. Nonetheless, the recent combination of datasets presented by the Dark Energy Spectroscopic Instrument (DESI) collaboration [1], including their new data release on Baryon Acoustic Oscillations (BAO) together with the Planck CMB 2018 data [2] (the *Plik*, *Commander*, and *SimAll* likelihoods based on the 2018 PR3 dataset on Temperature and Polarization, together with the *NPIPE* PR4 Planck CMB lensing reconstruction [3] and the lensing data from the Data Release 6 of the Atacama Cosmology Telescope [4]), is showing only a (quite stringent) upper bound on the sum of neutrino masses,  $\sum m_\nu < 0.072$  eV [1], when imposing the most conservative prior  $\sum m_\nu > 0$ . There is no hint of a nonzero mass and the posterior probability actually shows a cusp at zero, so that the peak of the distribution, if extended with a Gaussian [5], would even go to (unphysical) negative values (see also [6]). Since positive neutrino masses imply a suppression of the matter power spectrum, this would mean that such data prefer an enhancement of the spectrum.

However, it is known that this preference in the direction of negative values is correlated to the lensing “anomaly,” or tension, present in the likelihoods based on Planck 2018 data [2], i.e. the fact that the ad

hoc parameter  $A_L$ , that rescales the deflection power spectrum used to lens the primordial CMB power spectra, is larger than 1 when it is left free to vary, instead of being consistent with its real value  $A_L = 1$ . Forcing  $A_L = 1$  pushes instead the neutrino masses towards negative values [2]. Recently, new likelihoods for the final (PR4) Planck CMB data release have been published [7], both for high- $\ell$  TT, TE and EE spectra (HiLLiPoP) and for the low- $\ell$  EE polarization spectra (LoLLiPoP), to be used together with the Planck18 low- $\ell$  TT data. Such new likelihoods have been shown to lead to  $A_L = 1.039 \pm 0.052$  in  $\Lambda$ CDM, consistent with the expected value of unity. It has been already shown using CMB data alone [7], that as a result of this shift, the neutrino masses move to more positive values.

The aim of this *Letter* is to assess the status of the preference for positive neutrino masses employing such new CMB likelihoods, combined together with the new released BAO data from galaxies and quasars [8] at redshifts  $0.3 \lesssim z \lesssim 1.5$  and from the Lyman- $\alpha$  forest [9] by DESI [1] 2024. We will also check the impact on neutrino masses of Supernovae datasets, i.e. *Pantheon+* [10] and *DES-SN5YR* [11].

We will analyse such bounds in the context of the  $\Lambda$ CDM model, with varying neutrino masses. Subsequently, we will also consider neutrino mass bounds in extensions of the  $\Lambda$ CDM model that have been recently proposed to address the Hubble tension with the addition of a Dark Radiation (DR) component [12].

In all the analyses, we will apply a prior  $\sum m_\nu > 0$ , i.e. we assume here no prior information from neutrino oscillation experiments, in order to have a fully

\* itamar\_allali@brown.edu

† notari@fqa.ub.edu

independent measurement of neutrino masses.

## II. Models and datasets

We will first study the simple  $\Lambda$ CDM spatially-flat cosmological model with free sum of neutrino masses, the  $\Lambda$ CDM+ $\sum m_\nu$  model. We assume for simplicity the three neutrinos to have the same mass, since it has been shown that current experiments are sensitive only to the sum of neutrino masses, irrespective of how are they distributed [13].

We perform a Bayesian analysis using `CLASS` [14, 15] to solve for the cosmological evolution and either `MontePython` [16, 17] or `Cobaya` [18, 19] to collect Markov Chain Monte Carlo (MCMC) samples. We obtain posteriors and figures using `GetDist` [20]. We consider various combinations of datasets, as follows.

In Section III A we will explore three different Planck likelihoods for CMB data:

- **P18**: the Planck 2018 high- $\ell$  TT, TE, EE Plik, low- $\ell$  TT Commander, and low- $\ell$  EE SimAll likelihoods, together with the Planck 2018 lensing data [21];
- **P20<sub>H</sub>**: the HiLLiPoP + LoLLiPoP likelihoods [7], based on the final Planck data release (PR4) [22]. In particular: the HiLLiPoP likelihood at high- $\ell$  for TT, TE, EE; the LoLLiPoP likelihood for low- $\ell$  EE; the Planck 2018 Commander likelihood for low- $\ell$  TT and Planck 2018 CMB lensing data [21];
- **P20<sub>C</sub>**: The CamSpec likelihood [23], updated by [24] to the 2020 Planck PR4 data release [22], at high- $\ell$  for TT, TE, EE; the Planck 2018 Commander and SimAll likelihoods for low- $\ell$  TT and EE, respectively, and the Planck 2020 PR4 lensing likelihood [3].

Then, in Section III B, we will explore the effects of including different sets of cosmological supernovae:

- **Pantheon**: The Pantheon+ supernovae compilation [10].
- **DES-SN**: The DES-SN5YR supernovae compilation [11].

For most of this work, we will focus on the BAO measurements from DESI. In Section III C, we will also compare to other BAO measurements. The BAO datasets under consideration are:

- **DESI**: BAO measurements from DESI 2024 [1] at effective redshifts  $z = 0.3, 0.51, 0.71, 0.93, 1.32, 1.49, 2.33$ ;
- **SDSS<sub>16</sub>**: BAO measurements from 6dFGS at  $z = 0.106$  [25]; SDSS MGS at  $z = 0.15$  [26]; and SDSS

eBOSS DR16 measurements [5], including DR12 galaxies [27], and DR16 LRG [28, 29], QSO [30, 31], ELG [32, 33], Lyman- $\alpha$ , and Lyman- $\alpha \times$  QSO [34].

- **SDSS <sub>$f\sigma_8$</sub>** : The same BAO measurements given in **SDSS<sub>16</sub>**, while using the full-shape likelihoods for LRG, ELG, QSO, Lyman- $\alpha$ , and Lyman- $\alpha \times$  QSO [5], which include constraints on  $f\sigma_8$  from redshift-space distortions.
- **DESI/SDSS**: BAO measurements from the combination suggested in [1] that merges DESI 2024 with previous SDSS measurements, choosing for each bin the measurement with the highest precision to date.

After discussing the status of neutrino masses in the simplest setup, we will also extend our analysis to models beyond  $\Lambda$ CDM, that have recently been shown to address the so-called Hubble tension, i.e. the tension on the determination of the present Hubble rate from the above datasets with the following local direct measurement of the expansion rate by the SH0ES collaboration:

- **H<sub>0</sub>**: the measurement of the intrinsic SNIa magnitude  $M_b = -19.253 \pm 0.027$  [35], which uses a Cepheid-calibrated distance ladder. We add this always in combination with Pantheon+ data, as implemented in the Pantheon\_Plus\_SH0ES likelihood in MontePython.<sup>1</sup>

Such models extend  $\Lambda$ CDM by including a new Dark Radiation (DR) component, which lowers the tension [12], below  $3\sigma$  and as low as  $1.8\sigma$ , depending on the specific realization (free-streaming or fluid DR, present before BBN or produced after BBN<sup>2</sup>) and on the combination of datasets. Given the lower degree of tension, we are allowed in this case to combine with the **H<sub>0</sub>** measurement, interpreting the tension as a moderate statistical fluctuation. In Section IV, we will focus on one particular choice for the DR, the fluid DR present before the epoch of BBN, for simplicity.

## III. New constraints on neutrino masses in $\Lambda$ CDM+ $\sum m_\nu$

In this section we conservatively consider the  $\Lambda$ CDM model with variable neutrino masses, even if such model is: (1) in strong tension with SH0ES, and (2) mildly disfavoured compared to time varying dark-energy

<sup>1</sup> An even newer measurement from the collaboration is given in [36], but we use the value in [35] because of the available combination with Pantheon+.

<sup>2</sup> We note that constraints from primordial element abundances, which we do not include in this work, are not relevant when DR is produced after BBN.

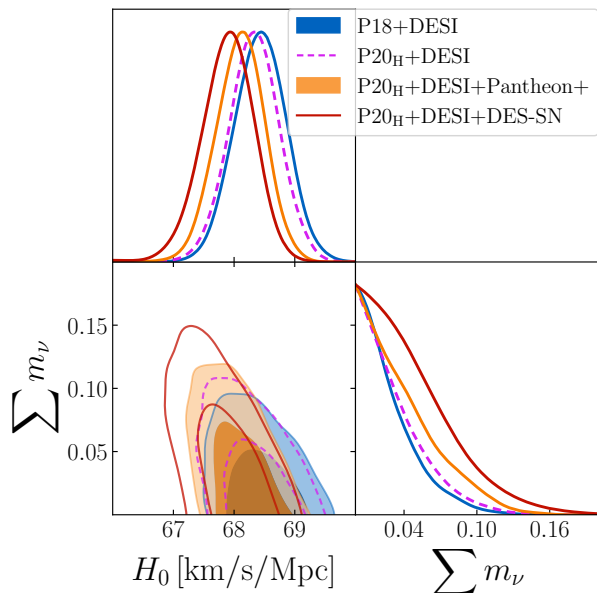


FIG. 1: One- and two-dimensional posteriors for  $H_0$  and  $\sum m_\nu$  in the  $\Lambda$ CDM +  $\sum m_\nu$  model, fitting to combinations of the Planck 2018 likelihoods with DESI BAO, compared to using the Planck 2020 HiLLiPoP+LoLLiPoP likelihoods with DESI BAO and the sets of cosmological supernovae from Pantheon+ and DES-SN5YR.

scenarios when not considering SH0ES (e.g. with respect to the so-called  $w_0w_a$ CDM model [1], which however points to the unphysical region with equation of state  $w < -1$ , or physically viable models, such as the “ramp” quintessence model [37]).

Within the  $\Lambda$ CDM+ $\sum m_\nu$  model, the DESI collaboration finds [1]  $\sum m_\nu < 0.072$  eV (95%CL, using DESI and Planck 2018 TT, TE, EE likelihoods, with PR4+ACT DR6 lensing data), which improves substantially on the analogous previous bound,  $\sum m_\nu < 0.12$  eV (95%CL, from Planck 2018 combined with SDSS DR12 BAO [2]). At face value, this new bound excludes the inverted hierarchy case ( $\sum m_\nu > 0.10$  eV) and starts to put some pressure even on the normal hierarchy case<sup>3</sup>. The situation, however, changes substantially when exploring various combinations of datasets, as discussed below.

### A. Effects of Planck Likelihoods

First, we discuss the effect of including more recent Planck likelihoods, from the PR4 2020 data release. The

<sup>3</sup> Note however that such a strong conclusion is not robust under the change of prior, i.e. it does not hold when using the prior based on neutrino oscillations,  $\sum m_\nu > 0.06$  eV.

Dataset	$\sum m_\nu$	Dataset	$\sum m_\nu$
<b>P18+DESI</b>	$< 0.077$	<b>P20<sub>C</sub>+DESI</b>	$< 0.080$
+ <b>Pantheon</b>	$< 0.086$	<b>P20<sub>H</sub>+SDSS<sub>16</sub></b>	$< 0.14$
+ <b>DES-SN</b>	$< 0.094$	<b>P20<sub>H</sub>+SDSS<sub>f\sigma_8</sub></b>	$< 0.11$
<b>P20<sub>H</sub>+DESI</b>	$< 0.086$	<b>P20<sub>H</sub>+DESI/SDSS</b>	$< 0.11$
+ <b>Pantheon</b>	$< 0.099$	+ <b>Pantheon</b>	$< 0.12$
+ <b>DES-SN</b>	$< 0.12$	+ <b>DES-SN</b>	$< 0.13$

TABLE I: 95%CL upper bounds on the neutrino mass sum for  $\Lambda$ CDM +  $\sum m_\nu$  model, comparing fits to various datasets.

bound gets substantially relaxed by making use of the recent HiLLiPoP+LoLLiPoP (**P20<sub>H</sub>**) likelihoods, leading to:

$$\sum m_\nu < 0.086 \text{ eV (95\%CL, P20}_H\text{+DESI)}.$$

The weakening of the bound compared to the case with **P18** is consistent with the expectation that a smaller  $A_L$  should lead to larger neutrino masses [7, 21, 38]. Note that we compare here to our **P18** combination which uses the Planck 2018 lensing, giving  $\sum m_\nu < 0.077$  eV (see Table I), rather than comparing to the constraint in [1] which uses a different lensing likelihood.

Using instead the CamSpec likelihood which has also been updated to PR4, we find an intermediate result:

$$\sum m_\nu < 0.080 \text{ eV (95\%CL, P20}_C\text{+DESI)}.$$

These constraints, as well the constraint from the combination of data **P18** defined above, are summarized in Table I. In addition, in Fig. 1, one can compare the posteriors of  $\sum m_\nu$  for **P18+DESI** and **P20<sub>H</sub>+DESI**, noting that the latter contour shows a relaxed constraint.

Since **P20<sub>H</sub>** and **P20<sub>C</sub>** use the most up-to-date set of data from Planck, and further, since it is has been shown that HiLLiPoP+LoLLiPoP have been the most effective at eliminating the  $A_L$  problem in the Planck data, we will take the combination **P20<sub>H</sub>** to be the preferred Planck dataset for the remainder of this work.

### B. Effects of Supernovae likelihoods

Adding supernovae, the bounds get further relaxed

$$\sum m_\nu < 0.099 \text{ eV (95\%CL, P20}_H\text{+DESI+Pantheon)},$$

$$\sum m_\nu < 0.12 \text{ eV (95\%CL, P20}_H\text{+DESI+DES-SN)}.$$

The fact that **DES-SN** leads to higher neutrino masses compared to **Pantheon** is consistent with the earlier analysis in [2]. Table I gives a summary of these constraints, including the combination of **P18** with supernovae data; we note that the addition of supernovae to **P18** has a similar shift to the replacement of **P18** by **P20<sub>H</sub>** (note also that this shift by adding Pantheon+ has been noticed in [39]).

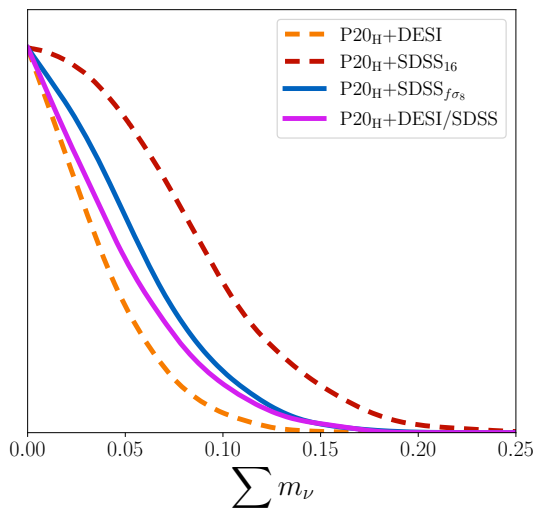


FIG. 2: One-dimensional posteriors for  $\sum m_\nu$ , fitting to combinations of **P20<sub>H</sub>** with different BAO datasets: **DESI**, **SDSS<sub>16</sub>**, **SDSS<sub>f $\sigma_8$</sub>** , or **DESI/SDSS**.

The resulting probability distributions are presented in Fig. 1. As one can see, the preferred neutrino masses move to more positive values compared to the **P18+DESI** case (see Appendix B), which looks promising in view of more precise measurements, from DESI or Euclid [40], that could finally confirm a detection of neutrino masses from cosmological data in the region allowed by oscillation experiments  $\sum m_\nu > 0.06$ . The inverted hierarchy scenario is also currently still allowed by the **P20<sub>H</sub>+DESI+DES-SN** combinations (and only marginally disfavored when considering **P20<sub>H</sub>+DESI+Pantheon**), even with the  $\sum m_\nu > 0$  prior.

We note that with supernovae data, the addition of more data provides a weaker bound, rather than a stronger one. This is an indication that the datasets in combination here are mildly in tension with respect to the effects of nonzero neutrino mass.

### C. Effects of BAO measurements

We also investigate here the effect of using other BAO datasets, instead of DESI. Using the most recent eBOSS DR16 measurements from SDSS [5] (in combination with 6DFGS [25] and older data from SDSS) the bound is substantially weaker:

$$\sum m_\nu < 0.14 \text{ eV (95\%CL, P20}_H\text{+SDSS}_{16}) .$$

The eBOSS BAO measurements can be also combined with  $f\sigma_8$  measurements from redshift-space distortions [5], which has more constraining power:

$$\sum m_\nu < 0.11 \text{ eV (95\%CL, P20}_H\text{+SDSS}_{f\sigma_8}) .$$

Finally, we used the combination of SDSS and DESI as described in [1], leading to

Dataset	$\sum m_\nu$
<b>P20<sub>H</sub>+DESI+Pantheon</b>	< 0.13
<b>P20<sub>H</sub>+DESI+Pantheon+H<sub>0</sub></b>	< 0.15
<b>P20<sub>H</sub>+DESI+DES-SN</b>	< 0.15
<b>P20<sub>H</sub>+DESI/SDSS+Pantheon</b>	< 0.15
<b>P20<sub>H</sub>+DESI/SDSS+DES-SN</b>	< 0.17

TABLE II: 95%CL upper bounds on the neutrino mass sum for the  $\Lambda$ CDM + Fluid DR +  $\sum m_\nu$  model, comparing different datasets.

$$\sum m_\nu < 0.11 \text{ eV (95\%CL, P20}_H\text{+DESI/SDSS}) .$$

This can be considered the state-of-the-art combination, since it uses the measurement with the best BAO statistical power in each redshift bin; this status will shift as DESI releases more data in the future. Note, however, that this combines data processed with different methods/pipelines, and the combination has not been fully validated. We can see here that, with this combination, both inverted and normal hierarchy for the neutrino mass are allowed at 95% confidence level.

## IV. Constraints on neutrino masses in extensions with Dark Radiation

Let us first point out the fact that, in  $\Lambda$ CDM, the sum of the neutrino masses is negatively correlated with  $H_0$ , as seen in Fig. 1. Thus, one may anticipate that a combined analysis with SH0ES would drive the fit towards smaller (or even negative, see [5, 6]) neutrino masses. This is precisely the case in  $\Lambda$ CDM, where it is actually inconsistent to combine with SH0ES (+**H<sub>0</sub>**; see Appendix A for further discussion of this effect).

On the other hand, in the Dark Radiation (DR) models which alleviate the Hubble tension [12], one may suspect that the same negative correlation exists. However, nonzero neutrino mass exhibits a slight positive correlation with the DR abundance  $\Delta N_{\text{eff}}$ , defined as the effective number of extra neutrino species  $\Delta N_{\text{eff}} \equiv \rho_{\text{DR}}/\rho_\nu$ , with  $\rho_{\text{DR}}$  and  $\rho_\nu$  being the energy densities of DR and one neutrino species, respectively. Since it is known that  $H_0$  and  $\Delta N_{\text{eff}}$  are positively correlated, the end result for the correlation of  $\sum m_\nu$  and  $H_0$  is not obvious.

We highlight the case of a perfect (self-interacting) fluid DR, over the case where DR is free-streaming, given that the fluid DR relaxes the Hubble tension more significantly [12]. We show results in Table II and in Fig. 3 for the fluid DR model across several datasets. We focus on the case where the fluid is present during the epoch of big-bang nucleosynthesis (BBN), but we have checked that the conclusions regarding neutrino mass are unaltered for the case where DR is produced after BBN.

Looking first at the constraints on the neutrino mass in Table II, we find overall larger values for the sum of neutrino masses within DR models compared to the



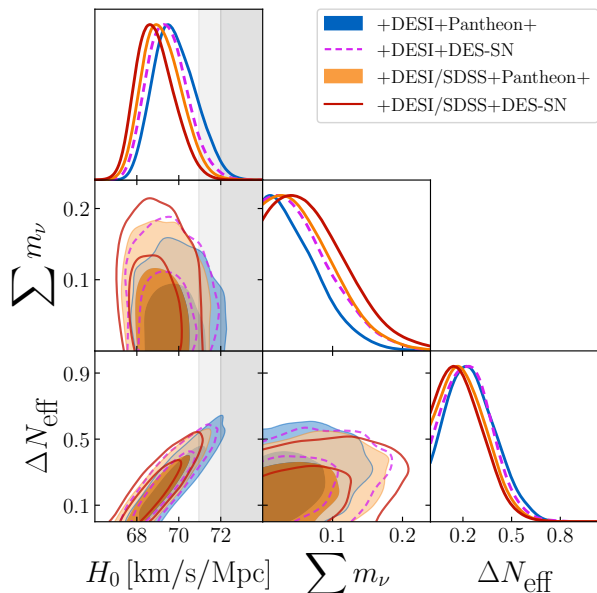


FIG. 3: One- and two-dimensional posteriors for  $H_0$ ,  $\sum m_\nu$ , and  $\Delta N_{\text{eff}}$  in the fluid DR model, fitting to combinations of **P20<sub>H</sub>** with either **DESI** or **DESI/SDSS**, and either **Pantheon** or **DES-SN**. The inner and outer two-dimensional contours give the 1- and 2- $\sigma$  confidence intervals, respectively. The dark and light gray bands show the 1- and 2- $\sigma$  confidence intervals from the measurement of  $H_0$  by the SH0ES collaboration.

$\Lambda$ CDM model.

Next, it can be appreciated in Fig. 3 that the degeneracy between  $H_0$  and  $\sum m_\nu$  exhibited in  $\Lambda$ CDM has been broken, and there is no longer a correlation. It is not surprising, therefore, that we see that the addition of the **H<sub>0</sub>** dataset does not substantially alter the neutrino mass bound in Table II (see Appendix A for further comparison). Moreover, we can see in Fig. 3 that the posteriors for  $\sum m_\nu$  are beginning to form peaks at nonzero values (see Appendix B for a discussion of the peak locations). For example, with the dataset **P20<sub>H</sub>+DESI/SDSS+DES-SN**, we see a clear peak in the posterior at a value  $\sum m_\nu \sim 0.04$  eV, which is  $< 0.5\sigma$  away from the expected value of 0.06 eV from neutrino oscillation experiments. Therefore, in the context of the fluid DR model as a solution to the Hubble tension, it is conceivable that a small increase in precision from upcoming data may also lead to the detection of neutrino masses. Note that all of the cases presented in Fig. 3 exhibit a  $< 3\sigma$  tension with SH0ES; however, the case with the highest neutrino masses also exhibits the highest

degree of tension with SH0ES, so it remains important to understand this interplay further.

## V. Conclusions

The new DESI 2024 data release, combined with Planck18 CMB data, at face value leads to a strong bound on neutrino masses in the  $\Lambda$ CDM model [1], when assuming a  $\sum m_\nu > 0$  prior, which excludes the inverted hierarchy scenario and seems to go even in the direction of negative masses [5, 6]. We have shown that these conclusions do *not* hold when using more recent Planck 2020 likelihoods (HiLLiPoP+LoLLiPoP), in combination with cosmological supernovae, since both go in the direction of favoring more positive masses. A conservative upper bound at 95%CL is indeed  $m_\nu < 0.12$  eV ( $m_\nu < 0.1$  eV) when adding also DES-SN5YR (or Pantheon+) supernovae.

Furthermore, we have analyzed neutrino mass bounds in a model with fluid Dark Radiation that addresses the Hubble tension [12], and we have shown that in this case: (i) neutrino mass bounds are driven to even larger values, (ii) bounds are robust when combining with the SH0ES measurement of  $H_0$ , and (iii) posterior probabilities even peak at nonzero neutrino masses.

Even if our findings go in the direction of relaxing constraints, they in fact constitute a significant improvement in the consistency with the expectation of  $\sum m_\nu \geq 0.06$  eV that comes from neutrino oscillation experiments. Overall, our results represent a promising starting point in the quest for neutrino mass detection with upcoming cosmological data.

## Acknowledgments

We thank Fabrizio Rompineve and Marko Simonovic for useful discussions. The work of A.N. is supported by the grants PID2019-108122GB-C32 from the Spanish Ministry of Science and Innovation, Unit of Excellence Maria de Maeztu 2020-2023 of ICCUB (CEX2019-000918-M) and AGAUR 2021 SGR 00872. The work of I.J.A. is supported by NASA grant 80NSSC22K081. A.N. is grateful to the Physics Department of the University of Florence for the hospitality during the course of this work. Part of this work was conducted using computational resources and services at the Center for Computation and Visualization, Brown University. We also acknowledge use of the INFN Florence cluster.

[1] A. G. Adame *et al.* (DESI), DESI 2024 VI: Cosmological Constraints from the Measurements of Baryon Acoustic Oscillations, (2024), [arXiv:2404.03002](https://arxiv.org/abs/2404.03002) [astro-ph.CO].

[2] N. Aghanim *et al.* (Planck), Planck 2018 results. VI. Cosmological parameters, *Astron. Astrophys.* **641**, A6 (2020), [Erratum: *Astron. Astrophys.* 652, C4 (2021)],

- arXiv:1807.06209 [astro-ph.CO].
- [3] J. Carron, M. Mirmelstein, and A. Lewis, CMB lensing from Planck PR4 maps, *JCAP* **09**, 039, arXiv:2206.07773 [astro-ph.CO].
  - [4] F. J. Qu *et al.* (ACT), The Atacama Cosmology Telescope: A Measurement of the DR6 CMB Lensing Power Spectrum and Its Implications for Structure Growth, *Astrophys. J.* **962**, 112 (2024), arXiv:2304.05202 [astro-ph.CO].
  - [5] S. Alam *et al.* (eBOSS), Completed SDSS-IV extended Baryon Oscillation Spectroscopic Survey: Cosmological implications from two decades of spectroscopic surveys at the Apache Point Observatory, *Phys. Rev. D* **103**, 083533 (2021), arXiv:2007.08991 [astro-ph.CO].
  - [6] N. Craig, D. Green, J. Meyers, and S. Rajendran, No *vs* is Good News, (2024), arXiv:2405.00836 [astro-ph.CO].
  - [7] M. Tristram *et al.*, Cosmological parameters derived from the final Planck data release (PR4), *Astron. Astrophys.* **682**, A37 (2024), arXiv:2309.10034 [astro-ph.CO].
  - [8] A. G. Adame *et al.* (DESI), DESI 2024 III: Baryon Acoustic Oscillations from Galaxies and Quasars, (2024), arXiv:2404.03000 [astro-ph.CO].
  - [9] A. G. Adame *et al.* (DESI), DESI 2024 IV: Baryon Acoustic Oscillations from the Lyman Alpha Forest, (2024), arXiv:2404.03001 [astro-ph.CO].
  - [10] D. Scolnic *et al.*, The Pantheon+ Analysis: The Full Data Set and Light-curve Release, *Astrophys. J.* **938**, 113 (2022), arXiv:2112.03863 [astro-ph.CO].
  - [11] T. M. C. Abbott *et al.* (DES), The Dark Energy Survey: Cosmology Results With  $\sim 1500$  New High-redshift Type Ia Supernovae Using The Full 5-year Dataset, (2024), arXiv:2401.02929 [astro-ph.CO].
  - [12] I. J. Allali, A. Notari, and F. Rompineve, Dark Radiation with Baryon Acoustic Oscillations from DESI 2024 and the  $H_0$  tension, (2024), arXiv:2404.15220 [astro-ph.CO].
  - [13] E. Di Valentino *et al.* (CORE), Exploring cosmic origins with CORE: Cosmological parameters, *JCAP* **04**, 017, arXiv:1612.00021 [astro-ph.CO].
  - [14] J. Lesgourgues, The Cosmic Linear Anisotropy Solving System (CLASS) I: Overview, (2011), arXiv:1104.2932 [astro-ph.IM].
  - [15] D. Blas, J. Lesgourgues, and T. Tram, The Cosmic Linear Anisotropy Solving System (CLASS) II: Approximation schemes, *JCAP* **07**, 034, arXiv:1104.2933 [astro-ph.CO].
  - [16] B. Audren, J. Lesgourgues, K. Benabed, and S. Prunet, Conservative Constraints on Early Cosmology: an illustration of the Monte Python cosmological parameter inference code, *JCAP* **02**, 001, arXiv:1210.7183 [astro-ph.CO].
  - [17] T. Brinckmann and J. Lesgourgues, MontePython 3: boosted MCMC sampler and other features, *Phys. Dark Univ.* **24**, 100260 (2019), arXiv:1804.07261 [astro-ph.CO].
  - [18] J. Torrado and A. Lewis, Cobaya: Code for Bayesian Analysis of hierarchical physical models, *JCAP* **05**, 057, arXiv:2005.05290 [astro-ph.IM].
  - [19] J. Torrado and A. Lewis, Cobaya: Bayesian analysis in cosmology, Astrophysics Source Code Library, record ascl:1910.019 (2019).
  - [20] A. Lewis, GetDist: a Python package for analysing Monte Carlo samples, (2019), arXiv:1910.13970 [astro-ph.IM].
  - [21] N. Aghanim *et al.* (Planck), Planck 2018 results. V. CMB power spectra and likelihoods, *Astron. Astrophys.* **641**, A5 (2020), arXiv:1907.12875 [astro-ph.CO].
  - [22] Y. Akrami *et al.* (Planck), Planck intermediate results. LVII. Joint Planck LFI and HFI data processing, *Astron. Astrophys.* **643**, A42 (2020), arXiv:2007.04997 [astro-ph.CO].
  - [23] G. Efstathiou and S. Gratton, A Detailed Description of the CamSpec Likelihood Pipeline and a Reanalysis of the Planck High Frequency Maps 10.21105/astro.1910.00483 (2019), arXiv:1910.00483 [astro-ph.CO].
  - [24] E. Rosenberg, S. Gratton, and G. Efstathiou, CMB power spectra and cosmological parameters from Planck PR4 with CamSpec, *Mon. Not. Roy. Astron. Soc.* **517**, 4620 (2022), arXiv:2205.10869 [astro-ph.CO].
  - [25] F. Beutler, C. Blake, M. Colless, D. H. Jones, L. Staveley-Smith, L. Campbell, Q. Parker, W. Saunders, and F. Watson, The 6dF Galaxy Survey: Baryon Acoustic Oscillations and the Local Hubble Constant, *Mon. Not. Roy. Astron. Soc.* **416**, 3017 (2011), arXiv:1106.3366 [astro-ph.CO].
  - [26] A. J. Ross, L. Samushia, C. Howlett, W. J. Percival, A. Burden, and M. Manera, The clustering of the SDSS DR7 main Galaxy sample – I. A 4 per cent distance measure at  $z = 0.15$ , *Mon. Not. Roy. Astron. Soc.* **449**, 835 (2015), arXiv:1409.3242 [astro-ph.CO].
  - [27] S. Alam *et al.* (BOSS), The clustering of galaxies in the completed SDSS-III Baryon Oscillation Spectroscopic Survey: cosmological analysis of the DR12 galaxy sample, *Mon. Not. Roy. Astron. Soc.* **470**, 2617 (2017), arXiv:1607.03155 [astro-ph.CO].
  - [28] J. E. Bautista *et al.* (eBOSS), The Completed SDSS-IV extended Baryon Oscillation Spectroscopic Survey: measurement of the BAO and growth rate of structure of the luminous red galaxy sample from the anisotropic correlation function between redshifts 0.6 and 1, *Mon. Not. Roy. Astron. Soc.* **500**, 736 (2020), arXiv:2007.08993 [astro-ph.CO].
  - [29] H. Gil-Marín *et al.* (eBOSS), The Completed SDSS-IV extended Baryon Oscillation Spectroscopic Survey: measurement of the BAO and growth rate of structure of the luminous red galaxy sample from the anisotropic power spectrum between redshifts 0.6 and 1.0, *Mon. Not. Roy. Astron. Soc.* **498**, 2492 (2020), arXiv:2007.08994 [astro-ph.CO].
  - [30] J. Hou *et al.* (eBOSS), The Completed SDSS-IV extended Baryon Oscillation Spectroscopic Survey: BAO and RSD measurements from anisotropic clustering analysis of the Quasar Sample in configuration space between redshift 0.8 and 2.2, *Mon. Not. Roy. Astron. Soc.* **500**, 1201 (2020), arXiv:2007.08998 [astro-ph.CO].
  - [31] R. Neveux *et al.* (eBOSS), The completed SDSS-IV extended Baryon Oscillation Spectroscopic Survey: BAO and RSD measurements from the anisotropic power spectrum of the quasar sample between redshift 0.8 and 2.2, *Mon. Not. Roy. Astron. Soc.* **499**, 210 (2020), arXiv:2007.08999 [astro-ph.CO].
  - [32] A. Tamone *et al.* (eBOSS), The Completed SDSS-IV extended Baryon Oscillation Spectroscopic Survey: Growth rate of structure measurement from anisotropic clustering analysis in configuration space between redshift 0.6 and 1.1 for the Emission Line Galaxy sample, *Mon. Not. Roy. Astron. Soc.* **499**, 5527 (2020), arXiv:2007.09009 [astro-ph.CO].
  - [33] A. de Mattia *et al.* (eBOSS), The Completed SDSS-IV extended Baryon Oscillation Spectroscopic Survey: measurement of the BAO and growth rate of structure

- of the emission line galaxy sample from the anisotropic power spectrum between redshift 0.6 and 1.1, *Mon. Not. Roy. Astron. Soc.* **501**, 5616 (2021), [arXiv:2007.09008 \[astro-ph.CO\]](#).
- [34] H. du Mas des Bourboux *et al.* (eBOSS), The Completed SDSS-IV Extended Baryon Oscillation Spectroscopic Survey: Baryon Acoustic Oscillations with Ly $\alpha$  Forests, *Astrophys. J.* **901**, 153 (2020), [arXiv:2007.08995 \[astro-ph.CO\]](#).
- [35] A. G. Riess *et al.*, A Comprehensive Measurement of the Local Value of the Hubble Constant with 1 km s $^{-1}$  Mpc $^{-1}$  Uncertainty from the Hubble Space Telescope and the SH0ES Team, *Astrophys. J. Lett.* **934**, L7 (2022), [arXiv:2112.04510 \[astro-ph.CO\]](#).
- [36] L. Breuval, A. G. Riess, S. Casertano, W. Yuan, L. M. Macri, M. Romaniello, Y. S. Murakami, D. Scolnic, G. S. Anand, and I. Soszyński, Small Magellanic Cloud Cepheids Observed with the Hubble Space Telescope Provide a New Anchor for the SH0ES Distance Ladder, (2024), [arXiv:2404.08038 \[astro-ph.CO\]](#).
- [37] A. Notari, M. Redi, and A. Tesi, Consistent Theories for the DESI dark energy fit, (2024), [arXiv:2406.08459 \[astro-ph.CO\]](#).
- [38] F. Couchot, S. Henrot-Versillé, O. Perdureau, S. Plaszczynski, B. Rouillé d'Orfeuill, M. Spinelli, and M. Tristram, Cosmological constraints on the neutrino mass including systematic uncertainties, *Astron. Astrophys.* **606**, A104 (2017), [arXiv:1703.10829 \[astro-ph.CO\]](#).
- [39] D. Wang, O. Mena, E. Di Valentino, and S. Gariazzo, Updating neutrino mass constraints with Background measurements, (2024), [arXiv:2405.03368 \[astro-ph.CO\]](#).
- [40] L. Amendola *et al.*, Cosmology and fundamental physics with the Euclid satellite, *Living Rev. Rel.* **21**, 2 (2018), [arXiv:1606.00180 \[astro-ph.CO\]](#).

## Appendix

### A. Combined analysis with SH0ES

Let us explore the effect of combining with SH0ES on neutrino masses.

First, in the context of  $\Lambda$ CDM, we can see in Fig. 4 that, due to the degeneracy between  $H_0$  and  $\sum m_\nu$ , a combination with SH0ES would cause a dramatically tighter constraint on  $\sum m_\nu$ . In this case, the would-be constraint from the combination **P20<sub>H</sub>+DESI+Pantheon+H<sub>0</sub>** is  $\sum m_\nu < 0.055$  eV, putting this constraint in conflict with neutrino oscillation experiments. Note that that the datasets in this combination are in great tension and therefore this combination is not justified.

Instead, in the case of fluid DR, the degeneracy between  $H_0$  and  $\sum m_\nu$  is no longer present. As seen in Table II, this means that the constraint on  $\sum m_\nu$  does not become tighter when adding SH0ES (now justified due to the lesser tension); in fact, it becomes even a bit weaker (shifting from  $< 0.13$  eV with **P20<sub>H</sub>+DESI+Pantheon** to  $< 0.15$  eV when adding **+H<sub>0</sub>**). Fig. 4 exhibits this as well, seen in the fact that the one-dimensional posterior for  $\sum m_\nu$  is not made tighter by SH0ES.

### B. Neutrino mass posteriors fit to a Gaussian

We discuss now an assessment of whether the neutrino mass posteriors are peaked at would-be negative values of the neutrino mass, as was considered in [5, 6]. To do so, we can take the posteriors which are inferred when using a prior of  $\sum m_\nu > 0$ , as we have done in this work, and fit them to the tail of a Gaussian. Then, one can project where the preferred peak would lie if the fit were to extend to negative masses. Note that in [6], a different method is proposed.

We see in Fig. 5 that for some datasets, the  $\Lambda$ CDM+ $\sum m_\nu$  model exhibits distributions that would peak at negative values. However, the inclusion of supernovae data drives these peaks closer to zero. Also, when combining the DESI BAO and SDSS BAO measurements along with DES-SN5YR supernovae, we can see even a peak at positive values. Further, using the same technique underscores the fact that in the  $\Lambda$ CDM+ $\sum m_\nu$ + Fluid DR model, the peaks are definitively driven to positive values of  $\sum m_\nu$ .

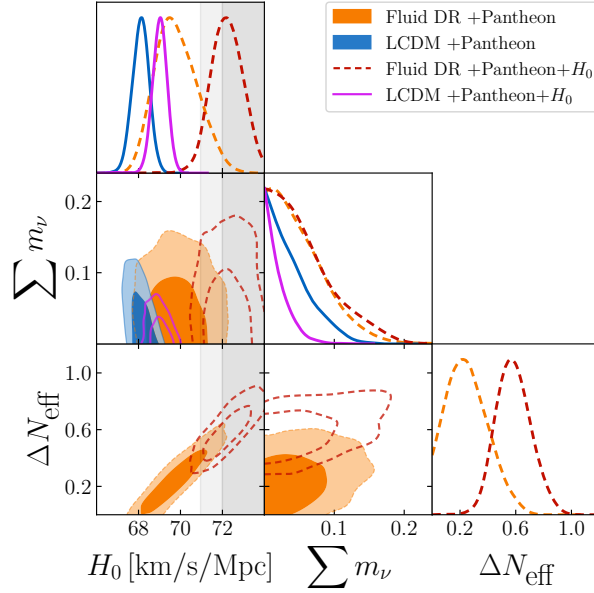


FIG. 4: One- and two-dimensional posteriors for  $H_0$ ,  $\sum m_\nu$ , and  $\Delta N_{\text{eff}}$  in both  $\Lambda$ CDM and the fluid DR model, fitting to **P20<sub>H</sub>+DESI+Pantheon** and the same set with the addition of **H<sub>0</sub>**. The inner and outer two-dimensional contours give the 1- and 2- $\sigma$  confidence intervals, respectively. The dark and light gray bands show the 1- and 2- $\sigma$  confidence intervals from the measurement of  $H_0$  by the SH0ES collaboration.

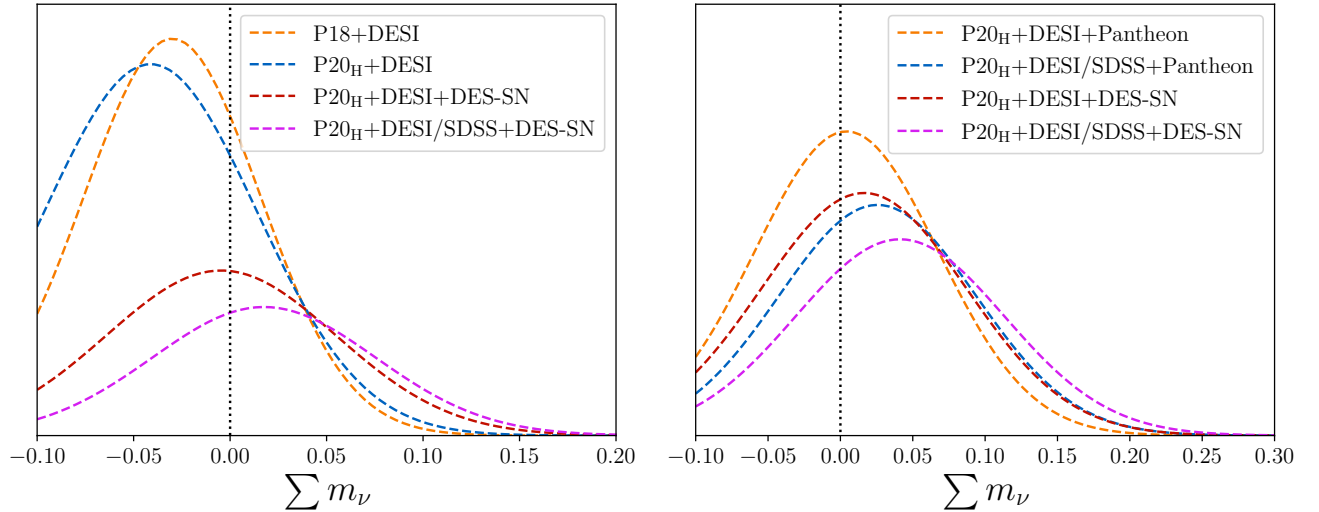


FIG. 5: Posterior distributions for  $\sum m_\nu$ , inferred with the prior  $\sum m_\nu > 0$ , are fit to Gaussian distributions and extended for  $\sum m_\nu < 0$  to project the approximate location of the peak preferred by the data. These curves are normalized such that the portion with  $\sum m_\nu > 0$ , corresponding to the posteriors from the MCMC analysis, integrates to unity. The left side figure shows various fits for the  $\Lambda$ CDM+ $\sum m_\nu$  model, while the right side shows the  $\Lambda$ CDM+ $\sum m_\nu$ + Fluid DR model.